

506089
12P
N92-120515
40257
P-11
PLANAR LASER IMAGING OF SPRAYS FOR LIQUID ROCKET STUDIES*

W. Lee, S. Pal, H. M. Ryan, P. A. Strakey and R. J. Santoro
Department of Mechanical Engineering
and
✓ NASA Propulsion Engineering Research Center
The Pennsylvania State University
University Park, PA

ABSTRACT

A planar laser imaging technique which incorporates an optical polarization ratio technique for droplet size measurement has been investigated. A series of pressure atomized water sprays have been studied with this technique and compared with measurements obtained using a Phase Doppler Particle Analyzer. In particular, the effects of assuming a logarithmic normal distribution function for the droplet size distribution within a spray has been evaluated. Reasonable agreement between the instruments has been obtained for the geometric mean diameter of the droplet distribution. However, comparisons based on the Sauter mean diameter show larger discrepancies, essentially because of uncertainties in the appropriate standard deviation to be applied for the polarization ratio technique. Comparisons have also been made between single laser pulse (temporally resolved) measurements with multiple laser pulse visualizations of the spray.

INTRODUCTION

Spray and droplet measurements in liquid rocket engines require non-intrusive techniques which possess both high spatial and temporal resolution capabilities. In addition, due to the short duration and highly transient nature of liquid rocket combustion processes, techniques which provide extensive spatial measurement capabilities are highly desirable. Recent progress in the development of planar laser imaging techniques have demonstrated the potential for achieving such measurements^{1,2}. In the present work, a planar laser imaging approach which incorporates an optical polarization ratio technique has been investigated as a spray diagnostic for sizing droplets. A series of pressure atomized water sprays have been imaged to obtain droplet size. These measurements have been compared with results obtained with a Phase Doppler Particle Analyzer (PDPA) for the same sprays.

Previous studies employing the polarization ratio approach for point measurements in sprays have observed smaller droplet sizes than typically reported for other measurement techniques^{3,4}. Since the polarization ratio technique requires an assumption regarding the droplet size distribution, this aspect of the problem has been selected for specific investigation. The present study has focussed on a logarithmic normal representation of the droplet size distribution, since some of the previous studies using the polarization ratio technique have used this distribution in their analysis of the droplet measurements^{3,4}. Using the information on the droplet size distribution provided by the PDPA measurements, detailed comparisons have been made to analyze the effects of variations in the geometric mean standard deviation of the logarithmic normal distribution on the Sauter mean diameter results obtained from the polarization ratio measurements.

LIGHT SCATTERING THEORY

The droplet sizing technique selected for use in the present study involves measuring the ratio of the horizontal and vertical components of the scattered light intensity from a laser light sheet incident on the spray. The underlying physics of the light scattering process is described by Mie theory and has been

*Approved for public release; distribution unlimited.

extensively discussed in the literature with respect to applications to droplets⁵. Hence, only a brief summary of this measurement technique is provided here.

The scattering cross section for a droplet upon which light is incident is a function of the refractive index (m), the non-dimensional particle size ($X = \pi D/\lambda$) and the scattering angle (θ). The scattering angle is defined to be in the plane containing the incident light beam and the scattered light detector, and is measured with respect to the forward propagation direction of the incident light beam. The particle size dependence is reflected in the non-dimensional particle size parameter X which is proportional to the ratio of particle diameter (D) divided by the wavelength of the incident light (λ).

The power scattered into a unit solid angle can then be expressed as

$$P_{s,i} = I_{o,i} N C_{ij} (m, X, \theta) k \quad (1)$$

where $I_{o,i}$ is the incident power, N is the number of scatterers, C_{ij} is the scattering cross section and k is a constant which includes the effects of the optical probe volume and efficiency of the collection optics, detectors and detection electronics. The subscript i refers to the polarization component of the incident light which may be vertical (V) or horizontal (H).

The scatterers in a spray are not monodispersed, and therefore a size distribution effect must be included. A mean scattering cross section is obtained as

$$\bar{C}_{ij}(\theta) = \int P(D) C_{ij} (m, \pi D/\lambda, \theta) dD \quad (2)$$

Information on the particle size can be obtained separately from the effects of the number concentration (N) of scatterers if a ratio of the scattered intensity for two polarizations is obtained. The resulting polarization ratio, γ , is given by:

$$\gamma = (\bar{C}_{HH}/\bar{C}_{VV}) (\sin^2\phi/\cos^2\phi) \quad (3)$$

where ϕ is the angle between the polarization vector of the linearly polarized incident light and the horizontal plane, i.e., $I_{o,V} = I_o \sin^2\phi$ and $I_{o,H} = I_o \cos^2\phi$. It should be noted that the proportionality constant, k , and the number concentration cancel in this procedure. Since the volumetric scattering cross section $Q_{ij} = NC_{ij}$ is the quantity actually measured in the laboratory, the number concentration information can be obtained once the size of the particles has been established by using the measured intensity and the calculated mean scattering cross section. This requires that the scattering apparatus has been calibrated to determine k ⁶. If however, only size information is desired, no calibration is necessary.

For the polarization ratio measurement technique, previous workers^{3,4} have assumed the size distribution to be a logarithmic normal distribution with a geometric mean standard deviation, σ_g , equal to 0.28515. The argument behind using this distribution stems from the self-preserving size distribution which has previously been shown to closely describe a number of aerosol distributions. However, thorough measurements of actual local size distributions within a spray made with a Phase Doppler Particle Analyzer (to be discussed in a later section) show that this assumption is unfounded. The assumption of a logarithmic normal distribution within a spray is moderately realistic. However, the assumption of a unique value for the geometric mean standard deviation, σ_g , is unrealistic. Values of this parameter obtained throughout the spray show systematic variations from approximately 0.2 to 0.8. The systematic variations in σ_g alluded to here and its consequences on the polarization ratio measurement technique will be discussed in detail later.

The objective of the present investigation is to provide a diagnostic technique capable of measuring droplets in a combustng spray environment using a planar laser imaging approach. This necessitates a series of Mie scattering calculations of the polarization ratio for droplets. Since water was used for the experiments performed, a refractive index (m) of 1.33 was used for the calculations⁷. The Mie scattering calculations were carried out for a range of σ_g values for the logarithmic normal distribution and the results are depicted in Fig. 1. As the results indicate, the polarization ratio is a weak function of the geometric mean standard deviation, and hence only a single set of calculations for any realistic σ_g , as shown in Fig. 2, is necessary. The non-dimensional parameter X is varied from 10 to 1000 which corresponds to geometric mean diameters of 1.7 μm to 170 μm . The two decade variation of geometric mean diameter

corresponds to a decade reduction of the polarization ratio. Note that the results shown in these two figures have taken into account the finite angle over which scattered light is collected. For the present case, δ is $\pm 1^\circ$ for the experimental apparatus utilized in these studies as discussed in the next section. The inclusion of a finite collection angle for the scattering optics is important for the droplet calculations. For non-absorbing particles in the range of $1\ \mu\text{m}$ to $100\ \mu\text{m}$, the scattering cross section is observed to vary strongly as a function of collection angle. By carrying out the calculations over the actual collection angle, a better representation of the polarization ratio is thus achieved.

A 90° scattering angle for the collection optics was selected because of the convenience afforded by this arrangement for imaging studies. The finite angle over which scattered light is collected ($\pm 1^\circ$) was chosen as a compromise between the needed collected light intensity and the size sensitivity of the polarization ratio approach as determined from Mie theory. Other scattering and collection angles can be employed subject to the optical arrangement and measurement needs.

Based on the above analysis, a series of experiments have been conducted to determine the quantitative measurement capabilities of the polarization ratio technique for droplets.

EXPERIMENTAL

A water spray was used as a test case for validating the polarization ratio technique. The water spray emanated from a Delavan WDB 0.5 solid cone nozzle with a full cone spray angle of 30° . The flow rate of this nozzle is factory rated to be $525\ \text{mm}^3/\text{sec}$ (0.5 gallons per hour) at a differential pressure of 0.86 MPa (125 psig). The water spray was introduced vertically downward into a quiescent environment. Droplet size measurements at various positions within the spray were made using a Phase Doppler Particle Analyzer (PDPA) and the polarization ratio technique. Tests were performed at gauge pressures of 0.69 MPa (100 psig) and 1.03 MPa (150 psig). The following sections detail the experimental apparatus and setup of both the polarization ratio technique and the PDPA.

Polarization Ratio Technique

A schematic diagram of the apparatus used for the polarization ratio technique is shown in Fig. 3. A frequency-doubled Nd:YAG laser ($\lambda = 532\ \text{nm}$) with a pulse duration of 10 nsec was used to illuminate a thin slice along the central axis of the aforementioned water spray. The degree of randomly polarized light incident on the water spray was virtually eliminated by using a glan laser prism. By reducing the amount of randomly polarized light incident on the water spray, the ambiguity in measuring the polarization ratio is decreased. A half-wave plate was used to rotate the polarization vector of the incident laser beam to 45° with respect to the horizontal plane of polarization. Thus, equal intensities of horizontally and vertically polarized light illuminated the spray. The focussing and cylindrical lenses transformed the YAG doughnut beam into a thin two-dimensional laser sheet parallel and coincident with the nozzle's central axis.

Images of the scattered light intensity were obtained at a 90° scattering angle using a 350 mm macro-objective lens, a narrow bandpass filter (centered at 532 nm with a 1 nm bandwidth), a 50 mm by 50 mm cube beamsplitter, and two polarization filters. Calibrations of the cube beamsplitter showed that 8.7% more horizontally polarized light was transmitted than vertically polarized light. As a consequence of the biased beamsplitter, a correction factor was applied to one of the recorded scattered light images.

A pair of simultaneous images were taken with vertically and horizontally polarized scattered light using two 35 mm cameras and black and white film (Kodak TMAX 400). Simultaneous acquisition of the vertically and horizontally polarized scattered light images reduced the need for a spatially uniform laser sheet. Since a ratio of the scattered light intensity for each polarization is used for size determination, variations in the intensity cancel out providing the two images are properly aligned.

The linearity of the TMAX 400 film was evaluated for a particular developing time. The film was linear over a range of optical densities from 0.3 to 2.0. This density range corresponds to an exposure dynamic range of almost 1000. The slope of the optical density versus the log exposure curve for the film varies with the developing time. A detailed knowledge of the optical density versus log exposure curve becomes important when the scattered light images are transferred from the film negative with a solid state camera

to the imaging software.

The two 35 mm cameras were employed as a relatively inexpensive method for obtaining two simultaneous images. Additionally, the sensitivity of the 35 mm film is sufficient for the laser light scattering experiments, while providing higher resolution and a wider dynamic range than commonly available with solid state cameras. The high resolution characteristics of the film provide the potential to enlarge portions of the negative for detailed analysis. The use of photographic film, however, introduces some disadvantages. This method is not a real time process, and therefore, an interactive experiment is not possible. In addition, transferring an image from film to an image processor complicates the procedure and introduces the potential for degradation of the image.

The images on the negative films were digitized using a CID solid state camera with a resolution of 512 by 512 pixels and a frame grabber. The digitized images were analyzed using an IBM AT compatible computer and the two-dimensional polarization ratio results were calculated from a pair of vertically and horizontally polarized scattered light images.

Two types of spray images were taken. The first being a single laser shot image where only a single laser pulse was allowed to illuminate the spray (one 10 nsec laser pulse). The second being a multiple exposure image where 80 laser pulses were used to image the spray on the pair of negatives. The impetus behind the multiple exposure image was to obtain an average droplet size over many realizations that could be compared with the PDPA measurements. The choice of a multiple exposure of 80 laser pulses was a compromise between obtaining an average droplet size and maintaining reasonable film resolution. Note that the single shot image essentially freezes the water spray in time, yielding an instantaneous droplet size measurement. Thus, one would expect more variation in the droplet size for the single shot images than for the multiple shot images.

Phase Doppler Particle Analyzer

Droplet size measurements in the water spray were made using the new Phase Doppler Particle Analyzer manufactured by Aerometrics, Inc.^{8,9} and represents an advancement over the previous counter processor instrument. The PDPA has been extensively used over the last decade^{10,11} and therefore, the theory behind the measurement technique is only discussed briefly. Both versions of the PDPA instrument measure the velocity and size of spherical, reflecting and/or refracting particles based on the same theoretical considerations. The advancement of the new PDPA model lies in the signal processing unit. The PDPA instrument extends the basic principles of the conventional dual beam Laser Doppler Velocimeter to obtain particle size in addition to velocity. A laser beam, an Argon-Ion beam in the present case, is split into two beams and focussed to an intersection to form a probe volume as shown in Fig. 4. A receiver system is located at some off-axis angle specifically chosen to best exploit the characteristics of the interference pattern of the particles of interest. For the case of water droplets, a 30° angle is most appropriate for detection of the interference pattern resulting from refraction of the laser light by the droplets. Note that the collection optics of the receiving system coupled with the transmitting optics define the probe volume characteristics. In addition to the collection optics, the receiving system consists of three detectors at appropriate separations to independently measure the "Doppler burst" signal from a particle traversing the probe volume. The three detectors measure the same burst signal, albeit with a phase shift. The velocity of the particle is then extracted from the temporal frequency of the burst signal, whereas the particle size is calculated from the measured phase shift between any two detectors and the a priori calculated linearity between the detector separation and the phase angle. The difference between the present model of the PDPA and previous versions lies in the signal processing. The signal processing for the counter processor system PDPA is done in the time domain, whereas for the new PDPA it is done in the frequency domain. It has been argued that the new PDPA is capable of better measurements in environments such as the dense spray region where the signal to noise ratio is extremely poor.⁸

RESULTS

In this section the results for both the PDPA and polarization ratio measurements of drop size are compared and discussed. Data is presented for a water spray issuing into a quiescent environment from a

Delavan WDB 0.5 solid cone nozzle having a full spray cone angle of 30°. The two test pressures used for these experiments were 0.69 MPa (100 psig) and 1.03 MPa (150 psig).

PDPA Measurements

The Phase Doppler Particle Analyzer (PDPA) with frequency domain signal processing was used to map out the drop sizes, specifically the Sauter mean diameter (D_{32}), within the spray for the Delavan nozzle. Drop size information in the form of histograms were obtained at ten equally spaced locations downstream of the nozzle ranging from 10 mm (0.39 inch) to 55 mm (2.2 inch). At each z location downstream of the nozzle, PDPA measurements of the drop size were made at equally spaced (2 mm (0.079 inch)) radial positions. The definition of the edge of the spray is a difficult quantity to determine and therefore the radial position was increased linearly until the data rate became extremely low.

Measurements of the diameter number distribution were made at each of the aforementioned grid locations. As a criteria, 8000 points were deemed to be necessary for providing reasonable accuracy for the diameter number distribution. Note that Lefebvre¹² suggests the use of at least 5500 data points for $\pm 5\%$ accuracy in the Sauter mean diameter measurements.

The PDPA is a point measurement technique and therefore the droplet size information is temporal in nature. The main purpose of this investigation is to determine the feasibility of the polarization ratio technique which measures spatially averaged droplet diameters. Therefore, all of the temporal measurements made with the PDPA were converted to yield spatially averaged droplet diameter distributions. Spatial Sauter mean diameters were calculated from the droplet distributions at each measurement location. Representative Sauter mean diameter measurements are presented and compared with polarization ratio technique measurements in the next section.

A goal of this investigation was to investigate the effects of the assumption regarding a logarithmic normal size distribution with a $\sigma_g = 0.28515$ within a spray which has been previously used by other investigators^{3,4}. To this end, the droplet size distribution at each measurement location was fit with a logarithmic normal distribution. The values of σ_g were seen to range from 0.2 to 0.8, with high values near the center of the spray and low values near the edges. It should be noted that the value of σ_g is not critical for the Mie scattering calculations as discussed earlier; however, it is critical in calculating any mean diameter for a logarithmic normal distribution. Any mean diameter of the form D_{pq} is related to the geometric mean diameter D_g in the following manner¹³:

$$D_{pq} = D_g \exp((p+q)\sigma_g^2/2) \quad (4)$$

A cursory examination of the above equation shows the sensitivity of σ_g in calculating higher moment diameters like the Sauter mean diameter from a logarithmic normal distribution.

As alluded to earlier, the observed variations of σ_g from high values near the center of the spray to low values towards the edges showed some general trends. It was therefore felt that a unique relationship probably existed between a local σ_g , the pressure ΔP , and both axial and radial locations within the spray. The experimental values of the local σ_g were found to best fit an expression of the following form

$$\sigma_g/\sigma_g|_{r=0} = A(r/\Delta P)^{-B} \quad (5)$$

away from the central core region of the spray. In the above expression, σ_g at any radial point is non-dimensionalized with the centerline value for the same axial location, and A and B are positive dimensional constants. The experimental data along with the least squares curve fit for the above equation is shown in Fig. 5. Note that for dimensional uniformity, the atmospheric pressure P_{atm} and the nozzle diameter D_{nozzle} are included in the relationship plotted in Fig. 5. The results indicate that in the core region of the spray, the use of a constant value for σ_g as shown in the figure is probably appropriate.

The implications of the results presented above on the analysis of the polarization ratio technique measurements are significant. Assuming a logarithmic normal distribution, the diameter that is directly measured with the polarization ratio technique is the geometric mean diameter D_g . Higher order diameters like D_{32} are then calculated uniquely using equation 4 with the correct local σ_g value, where σ_g can in turn be calculated independently with equation 5, provided the constants in the expression are known. It is

emphasized that the form of the equation relating the local value of σ_g to the location within a spray has by no means been universally proven and therefore extension to other types of sprays should be experimentally verified.

The previous discussion has concentrated on the variation of σ_g within a spray with the tacit assumption that the diameter is log-normally distributed. The assumption of a logarithmic normal diameter size distribution is now discussed. The PDPA measured values of the Sauter mean diameter (D_{32}) along with the calculated values of D_{32} using equation 4, for two axial locations are presented in Fig. 6. The agreement between the measurements and the calculations essentially represent the correlation coefficient of the least squares fit for the logarithmic normal distribution assumption. The conclusion from this figure (and others not presented here) is that the diameter distribution within a spray is more log-normally distributed near the edges than in the core region.

Polarization Ratio Technique Measurements

Both multiple (80 laser pulses) and single shot measurements of the water spray were taken and evaluated. A typical scattered light image of the water spray for the single exposure case is shown in Fig. 7 for the vertically polarized component of scattered light. Note that the image shows some structure and illustrates the high temporal resolution of this measurement approach. A similar image of the scattered light for the multiple exposure case is depicted in Fig. 8. Here, unlike the earlier image, the ensemble averaging of 80 images smoothes the irregularities in the spray and a uniform, symmetric spray structure is observed.

An estimate of the number density of droplets in most regions of the spray, especially near the outer edges, indicates that too few droplets are present to justify the calculation of the polarization ratio at the individual pixel level. Therefore, an 8x8 pixel matrix on the digitized images were averaged, yielding a spatial resolution of approximately 1 mm (0.039 inch) by 1 mm (0.039 inch). As a consequence of the pixel averaging, any error in aligning the two negatives of the scattered light components from the spray is minimized. These reduced resolution images were then used to calculate the polarization ratio.

An example of the polarization ratio obtained at the resolution level stated above is shown in Fig. 9. Qualitatively, a low polarization ratio translates to a high geometric mean diameter and vice versa as is readily discerned from Fig. 2. Therefore, using the gray level scale in Fig. 9, it is observed that the geometric mean diameter is small in the core region of the spray, and gradually increases outwards.

The geometric mean diameter D_g obtained using the polarization ratio technique and the PDPA instrument are compared in Figs. 10 and 11. Representative geometric mean diameter data at two locations, 30 mm (1.18 inch) and 50 mm (1.97 inch) downstream of the nozzle exit, and for a differential pressure of 0.69 MPa (100 psig) are only presented here. However, similar agreement was obtained for other spray locations and operating pressures. The radial extent of the polarization ratio measurements is smaller than the PDPA measurements because the low scattered light intensity near the extreme edges of the spray placed the results outside the film's linear range. Agreement between the two measurements (Fig. 10) is good near the core of the spray and within a factor of two for increasing radial distances. The trend of the D_g variation with radial distance for both measurement techniques is similar.

The single exposure polarization ratio measurements, plotted in Fig. 11, show the same trends in the D_g variation with considerably more scatter, a reflection of the instantaneous structures within the spray as also observed in Fig. 7.

The Sauter mean diameter D_{32} , which is of primary importance in combustion, obtained with the two techniques is presented in Fig. 12. Here it is noted that for the polarization ratio measurement, D_{32} is calculated from the measured value of D_g (Fig. 10) using equation 4 along with the appropriate curve fit value of σ_g (see eq. 5) as discussed earlier. Comparisons of D_{32} obtained from the two measurement techniques is within a factor of two (note that the D_{32} axis is offset from zero in the figure). The trend in D_{32} with radial distance is however not accurately followed and is a reflection of both differences in the D_g measurements and the highly sensitive dependence of the D_{32} calculation procedure on σ_g .

As the results indicate, the polarization ratio technique has some limitations. Simultaneous acquisition of measurements with high temporal and spatial resolution is unlikely to be achieved in low number density regions of the spray due to both the low intensity of scattered light and the statistically insignificant number of droplets present. Furthermore, in regions of the spray where D_g is less than 3 μm ,

the technique is inapplicable because of the multi-valuedness of the polarization ratio. Additionally, for multiple exposure conditions, information on σ_g is required from independent measurements. As a positive note, however, the present polarization ratio measurements do provide temporally and spatially resolved visualizations of sprays. The measurements quantitatively reflect the general size variations of D_g as a function of position and can provide spatially extensive information. Further developments using this techniques will require appropriate means to treat the droplet size distribution and the availability of wide dynamic range detection approaches.

SUMMARY

The quantitative measurement ability of the polarization ratio technique has been examined for a simple water spray. Specifically, measurements of the geometric mean and the Sauter mean diameter are compared with results from a Phase Doppler Particle Analyzer. Reasonable agreement for the spatial variation trends of D_g , the geometric mean diameter, between the two measurement techniques was observed. Sauter mean diameter (D_{32}) comparisons, however, highlighted the need to accurately know the standard deviation of the droplet size distribution for logarithmic normal representation. Future work should be directed towards examining other distributions such as the Rosin-Rammler¹⁴ or the Mukiyama-Tanasawa¹⁵. Finally, the present results support application of this technique to more complicated combustion environments for at least qualitative investigation of sprays^{16,17}. More quantitative applications will await advances which allows direct estimate of the size distribution function. This is an area of ongoing research.

ACKNOWLEDGEMENT

The authors would like to acknowledge the Penn State NASA Propulsion Engineering Research Center and Department of Energy through the Energy Conservation Utilization Technology Division for the support of this research.

REFERENCES

1. Hanson, R. K., "Combustion Diagnostics: Planar Imaging Techniques," Twenty-first Symposium (International) on Combustion, The Combustion Institute, Pittsburgh, PA, 1986, pp. 1677-1691.
2. Allen, M. G. and Hanson, R. K., "Digital Imaging of Species Concentration Fields in Spray Flames," Twenty-first Symposium (International) on Combustion, The Combustion Institute, Pittsburgh, PA, 1986, pp. 1755-1762.
3. Presser, C., Santoro, R. J., Semerjian, H. G. and Gupta, A. K., "Velocity and Droplet Size Measurements in a Fuel Spray," AIAA 24th Aerospace Sciences Meeting, Paper AIAA-86-0297, January 6-9, 1986, Reno, Nevada.
4. Presser, C., Gupta, A. K., Semerjian, H. G. and Santoro, R.J., "Application of Laser Diagnostic Techniques for the Examination of Liquid Fuel Spray Structure", Chem. Eng. Comm., 90, 1990, pp. 75-102.
5. Beretta, F., Cavaliere, A. and D'Alessio, A., "Drop Size and Concentration in a Spray by Sideward Laser Light Scattering Measurement," Comb. Sci. Tech., 36, 1984, pp. 19-37.
6. Santoro, R. J., Semerjian, H. G. and Dobbins, R. A., "Soot Particle Measurements in Diffusion Flames," Comb. and Flame, 51, 1983, pp. 203-218.
7. Bohren, C. F. and Huffman, D. R., Absorption and Scattering of Light by Small Particles, John Wiley and Sons, New York, NY, 1983, p 114.

8. Ibrahim, K. M., Werthimer, G. D. and Bachalo, W. D., "Signal Processing Considerations for Laser Doppler and Phase Doppler Applications," Presented at the Fifth International Symposium on the Application of Laser Techniques of Fluid Mechanics, Lisbon, Portugal, July 9-12, 1990.
9. Bachalo, W. D., Werthimer, G. D., Raffanti, R. and Hermes, R. J., "High Speed Doppler Signal Processor for Frequency and Phase Measurements," Aerometrics report 11-02.
10. Bachalo, W. D. and Houser, M. J., "Phase/Doppler Spray Analyzer for Simultaneous Measurements of Drop Size and Velocity Distributions," Optical Engineering, 23, 1984, pp. 583-590.
11. Dodge, L. G., "Comparison of Performance of Drop-Sizing Instruments," Applied Optics, 26, 1987, pp. 1328-1341.
12. Lefebvre, A. H., Atomization and Sprays, Hemisphere Publishing Corporation, Philadelphia, PA, 1989, p 370.
13. Dobbins, R. A., Santoro, R. J. and Semerjian, H. G., "Interpretation of Optical Measurements of Soot in Flames" in Combustion Diagnostics by Nonintrusive Methods, T. D. McCoy and J. A. Roux (editors), Progress in Astronautics and Aeronautics, vol. 92, 1984, pp. 208-237.
14. Rosin P. and Rammler, E., "The Laws Governing the Fineness of Powdered Coal," J. Inst. Fuel, Vol. 7, No. 31, 1933, pp. 29-36.
15. Nukiyama, S. and Tanasawa, Y., "Experiments on the Atomization of Liquids in an Air Stream," Report 3, On the Droplet-Size Distribution in an Atomized Jet, Defense Research Board, Department National Defense, Ottawa, Canada; translated from Trans. Soc. Mech. Eng. Jpn., " Vol. 5, No. 18, 1939, pp. 62-67.
16. Lee, W., Ryan, H. M., Strakey, P. A. and Santoro, R. J., "The Application of Two-Dimensional Imaging Techniques for Soot and Droplet Studies," to be presented at the 1990 ASME Winter Annual Meeting, Dallas, TX, November 25-30, 1990.
17. Cavaliere, A., Ragucci, R., D'Alessio, A. and Noviello, C., "Analysis of Diesel Sprays Through Two-Dimensional Laser Light Scattering," Twenty-second Symposium (International) on Combustion, The Combustion Institute, Pittsburgh, PA, 1988, pp. 1973-1981.

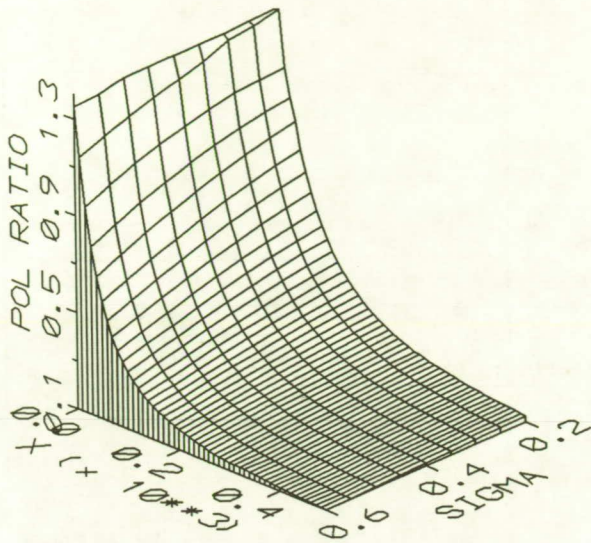


Fig. 1. Polarization ratio of scattered light calculated by Mie theory for a logarithmic normal distribution of water droplets as a function of the dimensionless size parameter, X , and the standard deviation, σ_g .

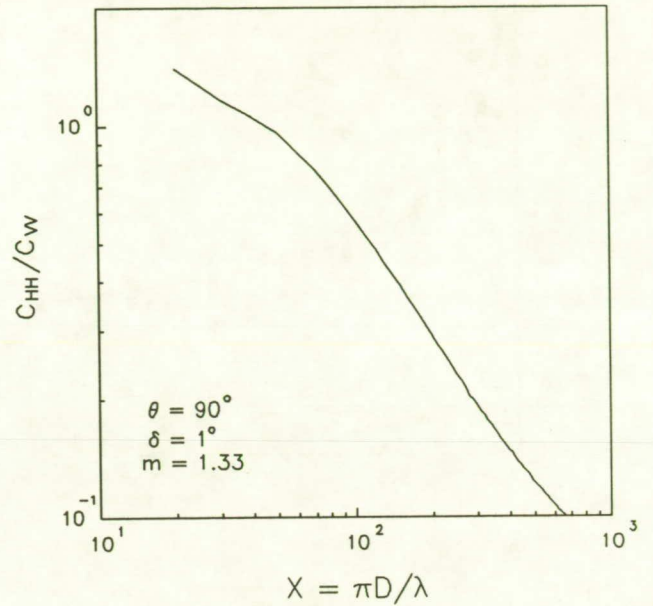


Fig. 2. Polarization ratio of scattered light calculated by Mie theory for a logarithmic normal distribution of water droplets as a function of the dimensionless size parameter, X .

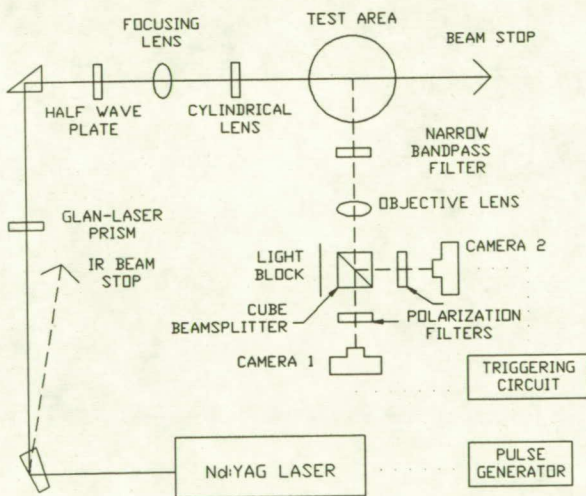


Fig. 3. Experimental setup for the polarization ratio technique.

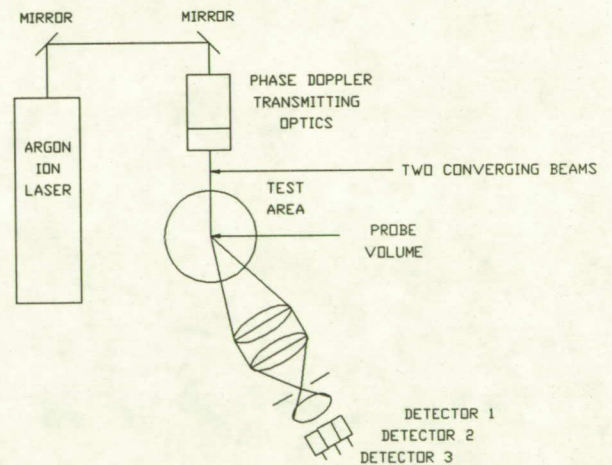


Fig. 4. Experimental setup for the Phase Doppler Particle Analyzer.

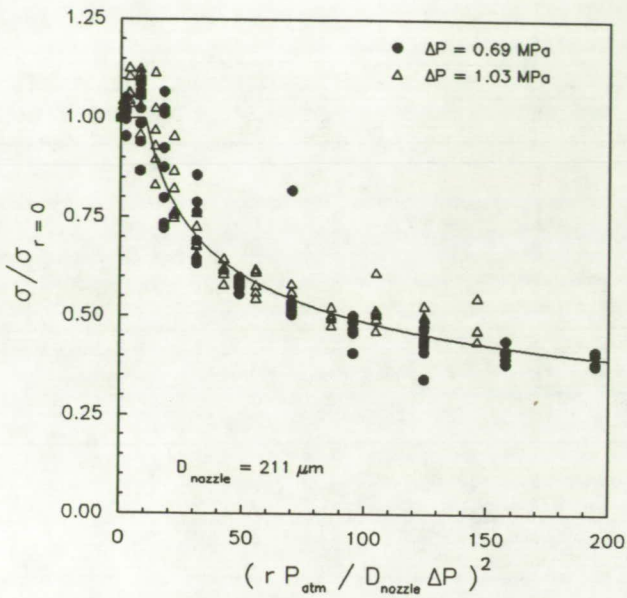


Fig. 5. Variation of the logarithmic normal standard deviation σ_g , normalized by the corresponding center line σ_g , versus a non-dimensionalized combination of the radial distance, r , and the pressure drop, ΔP , across the nozzle.

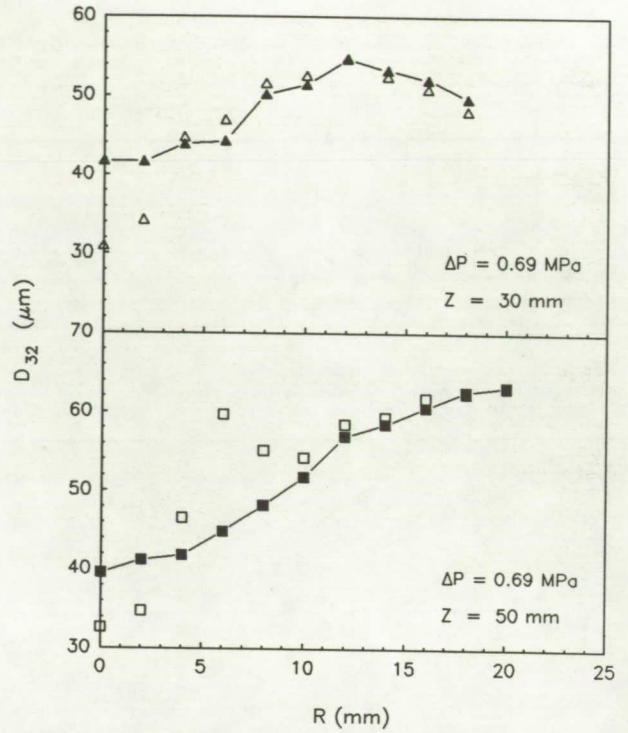


Fig. 6. Comparison of PDPA measured D_{32} (filled symbols) with D_{32} (open symbols) calculated using a logarithmic normal distribution.

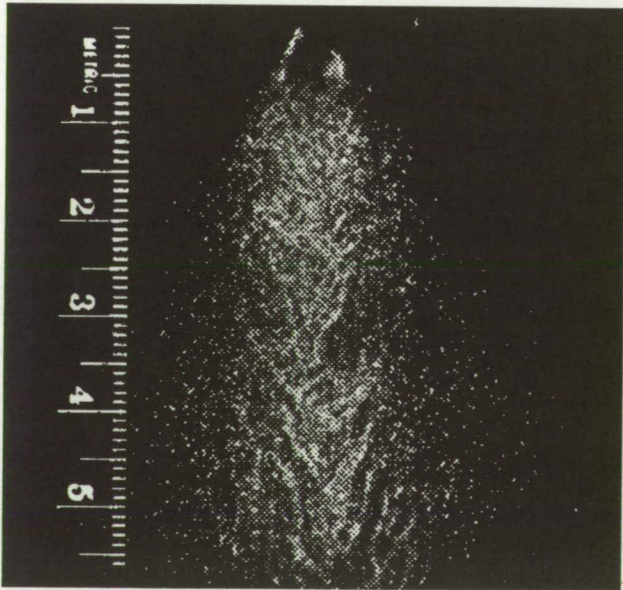


Fig. 7. Vertically polarized scattered light image of a water spray for a single exposure case from the solid state CID camera.

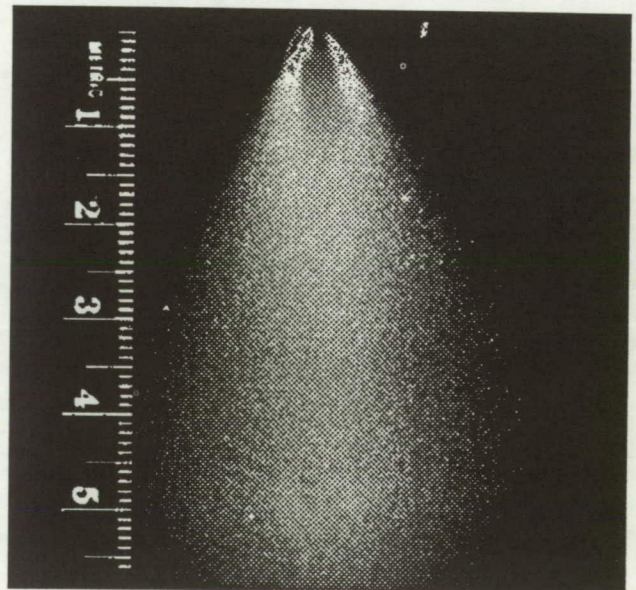


Fig. 8. Vertically polarized scattered light image of a water spray for a multiple (80) exposure case from the solid state CID camera.

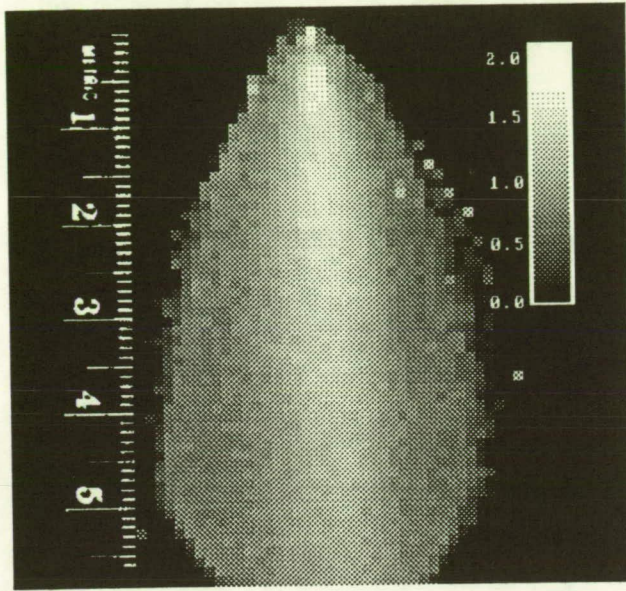


Fig. 9. Spatially averaged (8 x 8 pixels) polarization ratio obtained from simultaneous scattered light images with horizontal and vertical polarizations.

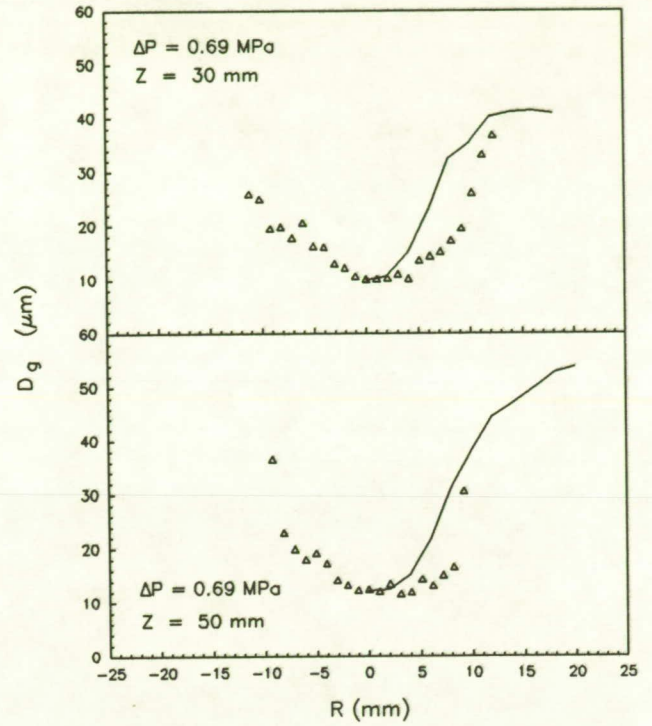


Fig. 10. Comparison of D_g measured by PDPA (—) with that measured by the polarization ratio technique (Δ) for a multiple (80) exposure case.

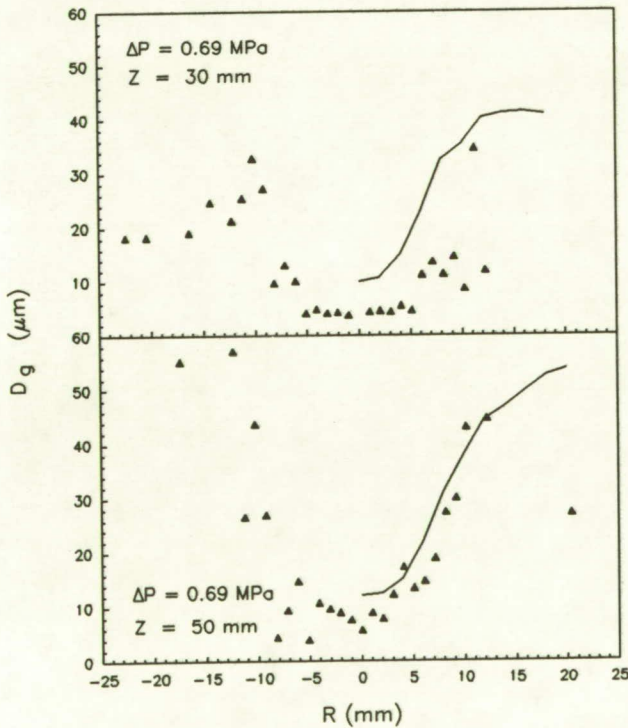


Fig. 11. Comparison of D_g measured by PDPA (—) with that measured by the polarization ratio technique (Δ) for a single exposure case.

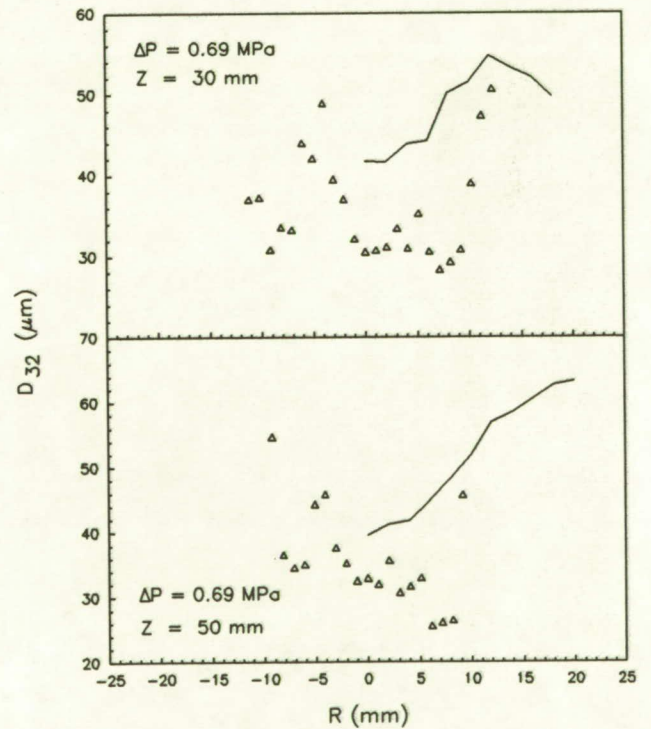


Fig. 12. Comparison of D_{32} measured by PDPA (—) with that measured by the polarization ratio technique (Δ) for a multiple (80) exposure case.